Journal of Environmental Protection, 2026, 17(9), 933-955
https://www.scirp.org/journal/jep
ISSN Online: 2152-2219
ISSN Print: 2152-2197

Integrating Segregated Subsurface Lithology into Aquifer Vulnerability Mapping: A Case Study of the Tochi Watershed

Joachim Bongomin[1], Geoffrey Openy[1], Denis Nono[1], Jimmy Byakatonda[1], Richard Louis Labeja[2], Martine Nyeko[1]

[1]Department of Biosystems Engineering, Gulu University, Gulu City, Uganda
[2]Department of Environment and Natural Resources Management, Gulu University, Gulu City, Uganda
Email: j.bongomin@gu.ac.ug

How to cite this paper: Bongomin, J., Openy, G., Nono, D., Byakatonda, J., Labeja, R.L. and Nyeko, M. (2026) Integrating Segregated Subsurface Lithology into Aquifer Vulnerability Mapping: A Case Study of the Tochi Watershed. *Journal of Environmental Protection*, **17**, 933-955.
https://doi.org/10.4236/jep.2026.179048

Received: July 29, 2026
Accepted: September 4, 2026
Published: September 7, 2026

Abstract

Aquifer vulnerability mapping is essential for protecting groundwater resources from contamination. This study aimed to enhance the accuracy of groundwater contamination risk zone delineation by introducing the use of segregated subsurface lithology. The study was conducted in Tochi watershed, in Northern Uganda. The vulnerability mapping using segregated lithology utilizes groundwater tables, land use, rainfall, and lithological data subdivided into soil, laterite, saprolite, and granite derived from borehole drill logs. The result of the vulnerability mapping based on segregated lithology was then compared with the one derived based on unsegregated lithology. Statistical analysis (T-test and one-sample t-test) revealed that the two methods produced statistically different vulnerability maps (P > Chi-square = 0). The segregated lithology approach demonstrated significant improvement in delineating high vulnerability zones (P-value = 0.0295) compared to the unsegregated method (P-value 0.47). It was also noted that the use of segregated lithology produced vulnerability zones with distinct partitioning with P-values = 0.00103 compared to unsegregated lithology approach, P-value = 0.07122. Overall accuracy, evaluated using the Area Under the Curve (AUC) based on the Groundwater Quality Index (GQI) of borehole wells for segregated lithology approach, showed good to very good model performance, accounting for 75% and 100% of areas under high and low potential, respectively. In consideration of factors such as Analytical Hierarchy Process (AHP) and criteria, the findings indicate that integrating segregated subsurface lithology provides a more distinct aquifer vulnerability partitioning that better conforms to GQI trends, offering a superior method for developing aquifer vulnerability maps and improving groundwater resource management. While GQI data suggest water sources are generally safe for the year ranging between 2003 and 2016 with 22% low risk, and 70.6% very low risk, the semi-confined nature of the aquifer and increasing anthropogenic activities necessitate improved mapping for future protection.

Keywords

Aquifer Vulnerability, Segregated Lithology, Subsurface Topology, Subsistence Agriculture, Groundwater Quality Index

1. Introduction

Groundwater is a vital resource, particularly in rural areas of developing nations, where it often serves as the primary source for domestic uses. However, these crucial resources are increasingly threatened by contamination, primarily driven by human activities and complex hydrogeological characteristics [1]. Factors such as shallow groundwater tables, permeable soils, and fractured bedrock can facilitate contaminant transport, overwhelming natural filtration processes [1], a situation further exacerbated by climate change [2]. Effective groundwater protection relies on accurate identification of contamination risk zones within watersheds. Vulnerability maps, generated through the overlay of various physical factors, are a common tool for this purpose [3]-[6]. Key parameters often include topography, lithology, depth to water table, rainfall, land use, conductivity, and vadose zone impact [7]. Among these, lithology and depth to water table are recognized as particularly sensitive factors determining aquifer vulnerability [8]. Despite its importance, previous studies have typically treated lithology as a single, homogeneous factor, often measured solely by hydraulic conductivity. This approach, however, inadequately captures the nuanced contribution of stratified subsurface layers to aquifer vulnerability. Stratified sublayers possess varied textural characteristics and spatial subsurface topologies, leading to diverse abilities to retain and transmit groundwater. These variations arise from differences in weathering processes within the Earth's crust, influencing vertical flow, lateral flow, and internal storage due to varied flow gradients. As demonstrated in our earlier findings [9], the variations alter flow convergence zones, a critical factor in aquifer vulnerability mapping and its partitioning. The spatial integration of each sublayer is thus hypothesized to result in a more accurate prediction of aquifer vulnerability. The present study aims to evaluate whether incorporating stratified lithological sublayers into aquifer vulnerability mapping enhances the accuracy of contamination risk assessment. By systematically testing the contribution of subsurface heterogeneity to flow convergence and aquifer susceptibility, the work seeks to establish the potential value of a segregated lithology approach in groundwater protection.

2. Study Area

The study was conducted in the Tochi watershed, located in Northern Uganda, as shown in **Figure 1**. The geology generally consists of sedimentary materials of igneous rock origin. Boreholes are the preferred source of water for most rural communities due to their safety. However, well contamination is being reported [10]. Those that have existed for a very long time have shown elevated biological and physical characteristics when compared to newly constructed ones [11]-[13]. Mixed land use exists within the watershed, with intensive subsistence agriculture practiced on predominantly sandy clay soil. This situation creates the possibility of pollutant transport to the shallow aquifer, necessitating the mapping of vulnerable areas [13].

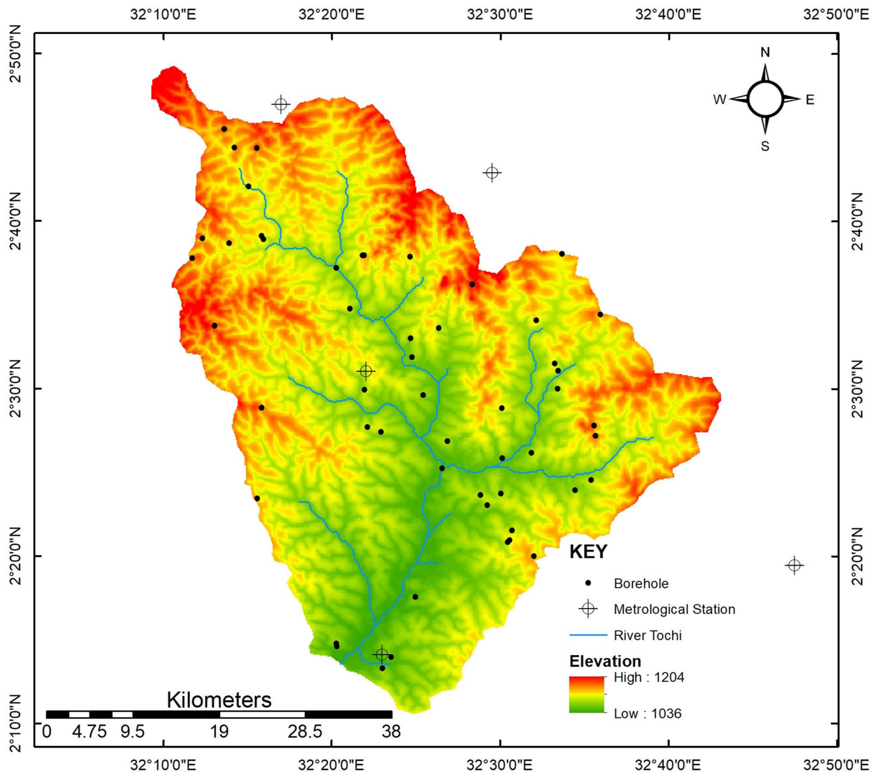

Figure 1. Map of the study area showing the spatial distribution of boreholes and meteorological stations.

3. Materials

Identification of aquifer vulnerability regions involved the use of factors such as groundwater table, land use, rainfall, and segregated lithology (soil, laterite, saprolite, and granite). Daily point data for production of the rainfall map were obtained from the NASA Power website (https://power.larc.nasa.gov/data-access-viewer/). The data period ranged between the years 1982 to 2023. Data from the Uganda Meteorological Authority for the same period were used to validate the satellite data. Land use data, with a 30-meter resolution, were obtained from the Earth Explorer website (https://earthexplorer.usgs.gov/) for the following paths and rows: path 171 row 058, path 172 row 058, and path 071 row 059. The acquired images were used to derive the land use map. The segregated lithology map was developed from the borehole drill logs in Geomodeller software from our previous study. 52 drill logs were used, with construction dates ranging between March 2003 and December 2016. The spatial distribution of boreholes within the watershed is one borehole per 42 square kilometers. The usable lithological intervals of the borehole in meters were as follows: soil (0 - 4), laterite (0 - 28), saprolite (0.3 - 40), and granite (13 - 65). The drill logs acquired from the districts of Gulu, Omoro, Nwoya, Oyam, and Apac were further used to develop the groundwater table map in ArcGIS.

4. Methods

Aquifer vulnerability mapping in this study used segregated and unsegregated lithologies presented as maps in addition to factors of groundwater table, land use, and rainfall. Segregated lithology was prepared using an implicit geo-modelling approach. The open lowest interval between 0 m and 67 m was used to construct the 3D model structure. The onlap relationship formed the basis for interpolation and segregation of sub-surfaces. The observed lithological depth from borehole logs formed the basis for segregation into layers with varying hydraulic properties and subsurface topology. The approach generated continuous topographic sub-surfaces from which a Digital Elevation Model (DEM) was developed. Reclassification of DEM generated lithological layers with varying vulnerability potential and score rating utilized in the Multicriteria Decision Method-Analytical Hierarchy Process (MCDM-AHP). Unsegregated lithology was generated through digitization of lithological boundaries from the Geology Map of Uganda-2008. The partitioning in the subsurface is assumed to follow the digitized boundaries. The digitized lithological boundaries were overlaid onto DEM, which formed the basis for reclassification into vulnerability potential. The core of our approach was to compare vulnerability classifications derived from two distinct lithological treatments: segregated and unsegregated. The land use map was generated through supervised classification of imagery generated using the Principal Component Analysis (PCA) method. The depth at which first water was struck during drilling operations was considered to represent the saturated zone and was used in this study to approximate groundwater table depth. The concept is supported by the aquifer system within the watershed characterized as semiconfined. Aquifer thickness purifies contaminants in infiltrated water through particle entrapment in void spaces or reaction of contaminants with lithology material through geochemical processes. A thick overburden provides more residence time within the medium for such processes to take place, thereby increasing purification likelihood before reaching the groundwater table. Groundwater table and rainfall maps were generated using kriging interpolation of depth to first water strike and annual rainfall received, respectively. The Groundwater Quality Index (GQI) was used to objectively interpret the results of the vulnerability mapping.

4.1. Vulnerability Mapping Using Segregated Lithology

Segregated lithologies are developed thematic maps of soil, laterite, saprolite, and granite. Within each lithological layer, hydraulic properties are assumed constant. Fissures within each lithological layer are also not accounted for within the sublayers generated. Water transmission potential in decreasing order is: saprolite, laterite, soil, and granite. The information is gathered through literature review on the hydraulic properties of segregated and unsegregated lithologies. Unsegregated lithology (Amuru group, gneissic granitoids of Uganda, and metagabbro) assumes uniform hydraulic properties for aquifer overburden, presenting a distinction in the method. Due to the limited information on stratification depth from the geology map of Uganda 2008, the spatial coverage of lithological boundaries is assumed to apply in the subsurface up to the water table. The decreasing order of water transmission potential is: Amuru group, gneissic granitoids of Uganda, and metagabbro, respectively. The lithological units were obtained through digitization of lithological boundaries. The water transmission potential, vulnerability potential, and score ratings were utilized in MCDM-AHP. A pairwise comparison matrix was generated by assigning scores (1.0 to 9.0) to selected factors, following guidelines established by [14]. This matrix was then normalized by dividing each value in a column by the sum of that column (Equation (1)). The weight of each factor was computed by averaging the sum of each row in the normalized pairwise comparison matrix (NPWM). A consistency check was performed (Equation (2) and Equation (3)) to ensure the reliability of the pairwise comparisons, with an acceptable Consistency Ratio (CR) of less than 0.1. For the 7 factors considered in this study, the corresponding random index (RI) was 1.32. Iterations were performed to adjust the CR value to an acceptable level.

$$\text{NPWM} = \frac{\text{Element of column}}{\text{Sum of column}} \quad (1)$$

$$\text{CI} = \frac{\lambda_{\max} - n}{n - 1} \quad (2)$$

$$\text{CR} = \frac{\text{CI}}{\text{RI}} \quad (3)$$

Where CI is the consistency index, n is the number of controlling factors to groundwater occurrence, λ is the highest eigenvalue of the pairwise matrix.

The weights generated through MCDM-AHP for production of the vulnerability map using segregated and unsegregated lithologies are shown in **Table 1** and **Table 2**, respectively. The corresponding consistency ratios (CRs) were 0.08 and 0.075. Vulnerability potential of land use was based on the extent to which the factor generates contaminants. The decreasing vulnerability potentials are: built-up land, subsistence agriculture, rangeland, wetland, plantation forest, and natural forest. The higher the potential, the higher the score rating assigned. Vulnerability potential of the groundwater table was interpreted in terms of aquifer thickness. Small depth means greater risk of contamination due to reduced residence time; therefore, a high score rating. Rainfall was interpreted in terms of the amount received. The higher the intensity, the greater the vulnerability potential, thus a high score rating. Segregated lithology was measured in terms of depth from the topographic land surface. Low depth means an increased chance of contaminant convergence, thus high vulnerability with a high score rating. The same procedure was applied in MCDM-AHP using unsegregated lithology.

Table 1. Weights used in MCDM-AHP for segregated lithology.

Factor	Classes	Recharge Potential	Weight (%)	Rating
Groundwater table (m)	16	High	5	4
	25	Low		3
	36	Very Low		2
	65	Extremely Low		1
Land use	Wetland	Low	10	3
	Natural forest	Extremely Low		1
	Plantation forest	Very Low		2
	Subsistence agriculture	Very High		5
	Rangeland	High		4
	Built up land	Extremely High		6
Rainfall (mm/month)	1053.3	Extremely Low	35	1
	1063.5	Very Low		2
	1073.8	Low		3
	1084.1	High		4
	1094.3	Very High		5
	1104.6	Extremely High		6
Soil (m)	25.9	Very High	15	5
	14.81	High		4
	9.3	Low		3
	0.8	Very Low		2
	0	Extremely Low		1
Laterite (m)	32	Extremely High	15	6
	26	Very High		5
	20.1	High		4
	14	Low		3
	7	Very Low		2
	2.2	Extremely Low		1
Saprolite (m)	46.8	Very High	14	5
	32.2	High		4
	20.2	Low		3
	7	Very Low		2
	0	Extremely Low		1
Granite (m)	74.9	Extremely High	8	6
	68.1	Very High		5
	61.3	High		4
	53	Low		3
	41.9	Very Low		2
	20.4	Extremely Low		1

Table 2. Weights used in MCDM-AHP for unsegregated lithology.

Factor	Class	Potential	Weight (%)	Rating
Groundwater table	16	High	7	4
	25	Low		3
	36	Very Low		2
	65	Extremely Low		1
Land use	Wetland	Low	15	3
	Natural forest	Extremely Low		1
	Plantation forest	Very Low		2
	Subsistence agriculture	Very High		5
	Rangeland	High		4
	Built up land	Extremely High		6
Rainfall	1053.3	Extremely Low	46	1
	1063.5	Very Low		2
	1073.8	Low		3
	1084.1	High		4
	1094.3	Very High		5
	1104.6	Extremely High		6
Amuru group	Not specified	High	9	4
		Low		3
		Very low		2
Gneissic granitoids of Uganda	Not specified	High	11	3
		Low		2
Metagabbro	Not specified	High	12	3
		Low		2

4.2. Overlay Operation to Produce Aquifer Vulnerability Map

The combination of the respective weight of each factor, vulnerability potential, and score ratings is utilized to produce a vulnerability map. The map is generated through the weighted overlay of developed thematic maps in ArcGIS according to Equation (4). The pixel values of the raster maps used in the overlay are multiplied by the respective weight influence obtained from AHP. Aquifer vulnerability is interpreted as a potential: high, low, and very low.

$$H = \sum_{i=1}^{7} x_i \cdot w_i \tag{4}$$

where H is the aquifer vulnerability map, i is the number of decision criteria, x_i is the particular normalized criterion, and w_i is the respective weight of the criterion.

4.3. Interpretation of Vulnerability Mapping Using the Groundwater Quality Index (GQI)

A one-sample test was conducted to determine if the two vulnerability maps (from segregated and unsegregated lithology) were statistically different. If no improvement was detected with segregated lithology, reclassification of thematic maps into finer intervals would have been performed. The Groundwater Quality Index (GQI) was used to evaluate variations between potential vulnerability categories and to assess the accuracy of both methods. Computation of GQI was based on secondary data from borehole water quality reports for the period March 2003 to December 2016. The water quality report was measured against the National Water and Sewerage Cooperation standard for potable water set by the Ministry of Water and Environment. The period was used because its data was readily available. Secondly, the historical contamination trend can still be used to determine the vulnerability mapping between the two methods. However, the data may not adequately represent the current contamination level within the watershed due to the cumulative effect arising from changing anthropogenic activities. The Arithmetic Water Quality Index (AWQI) method was employed to compute GQI, utilizing parameters such as pH, electrical conductivity (EC), apparent color, turbidity, Total Dissolved Solids (TDS), Total Suspended Solids (TSS), alkalinity (CaCO3 total), hardness, Ca^{2+}, bicarbonate as $CaCO_3^-$, chloride (Cl^-), fluoride (F), iron (total), sulphate, and nitrate. The AWQI was chosen for its broad applicability, simplicity, parameter flexibility, and ability to handle limited data. Quality ratings for each parameter were calculated using Equation (5) and for pH using Equation (6). Relative weights for each parameter were assigned based on their impact on human health (Equation (7)), and the GQI was computed using Equation (8).

$$Q_i = \frac{C_i}{S_i} \times 100\% \tag{5}$$

where Q_i is the quality rating, C_i is the concentration of the i^{th} measured parameter in groundwater, and S_i is the Uganda drinking water quality standard for the i^{th} parameter.

$$Q_{pH} = \frac{V_{pH} - 7.0}{S_{pH} - 7.0} \times 100\% \tag{6}$$

where V_{pH} is the observed pH and S_{pH} is the threshold value in the drinking water standard. For $V_{pH} > 7.0$, S_{pH} takes the upper limit value of pH, and for $V_{pH} < 7.0$, S_{pH} adopts the lower limit value of pH.

$$W_i = \frac{w_i}{\sum_{i=1}^{n} w_i} \tag{7}$$

where W_i is the relative weight of the i^{th} parameter, n is the number of parameters, and w_i is the weight of the ith parameter.

$$\mathrm{GQI} = \sum_{i=1}^{n} Q_i W_i \tag{8}$$

where GQI is the groundwater quality index, n is the number of parameters, Q_i is the quality rating of the i^{th} parameter, and W_i is the relative weight of the ith parameter.

The classified risk for each water point was imported into ArcGIS and overlaid onto the vulnerability maps for sorting into vulnerability classes for further analysis. A one-sample t-test was used to assess variation in vulnerability between the two methods using OriginPro software version 9.0.

5. Results

5.1. Vulnerability Mapping Criteria

1) Segregated Lithology

Vulnerability mapping was achieved using thematic maps presented in Figure 2. The lowest depth ranges representing regions of flow convergence are: soil 25.9 m to 14.8 m, laterite 32.0 m to 26.0 m, saprolite 61.4 m to 46.8 m, and granite 81.7 m to 74.9 m. Groundwater depths in the Tochi watershed ranged from a minimum of 6.1 m to a maximum of 64.9 m. Mixed land use, classified with 86.7% accuracy, exists within the watershed with respective spatial coverages of: subsistence agriculture (49.1%), rangeland (11.5%), built-up land (1.8%), wetland (34.6%), plantation forest (0.5%), and natural forest (2.5%). Annual rainfall varied from 1053.3 mm to 1104.6 mm. The accuracy of rainfall data used had a low Root Mean Square Error (RMSE) ranging between 0.073 and 0.332.

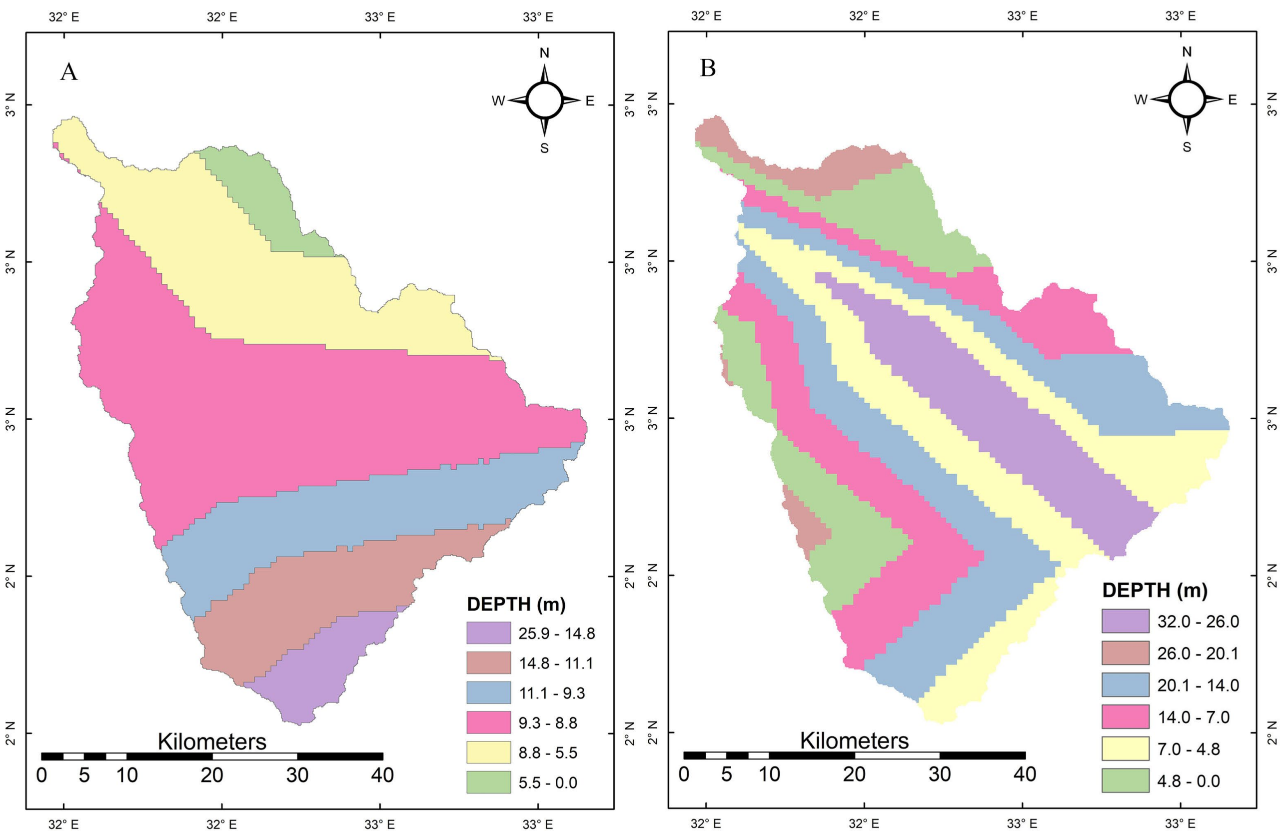

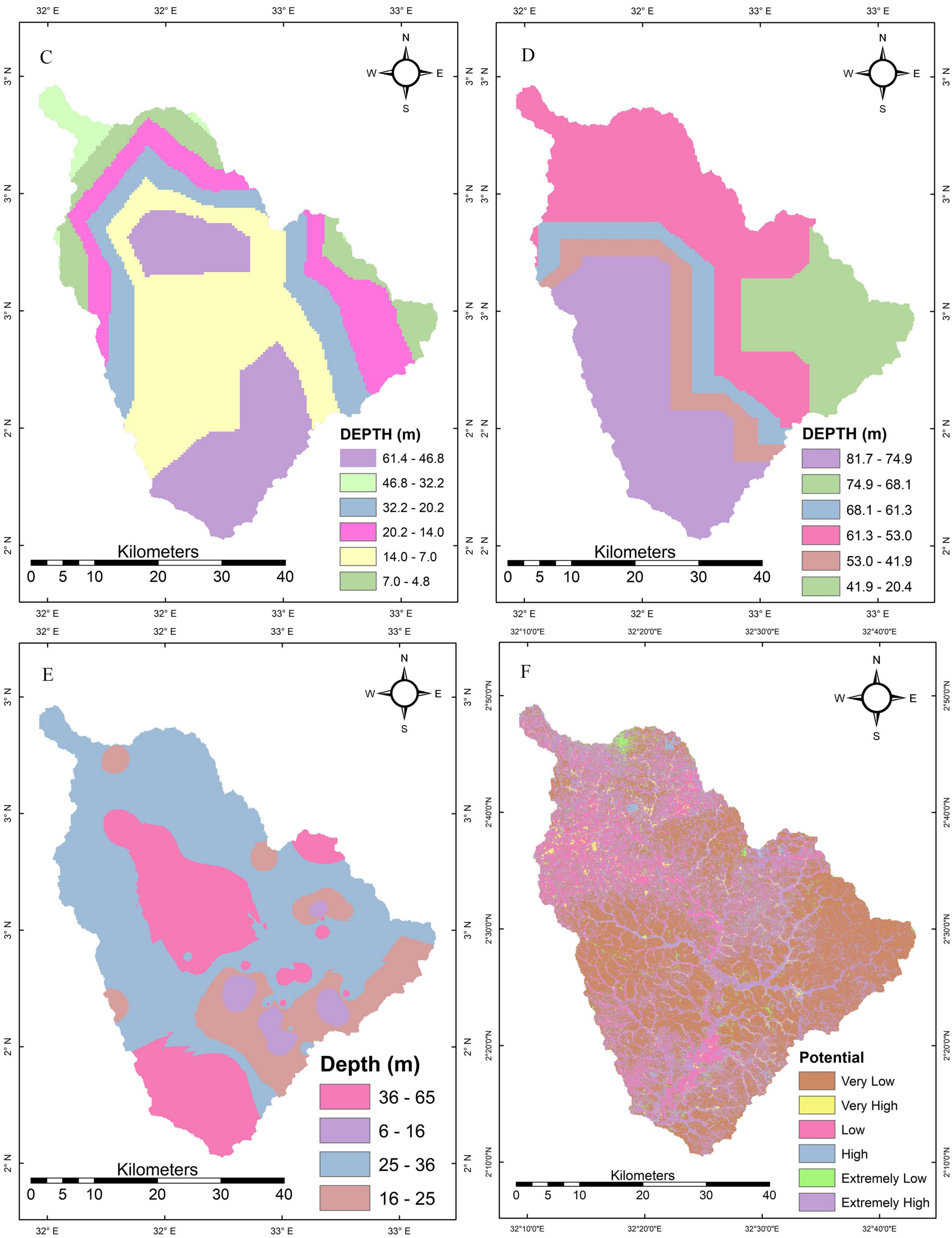
C
DEPTH (m)
61.4 - 46.8
46.8 - 32.2
32.2 - 20.2
20.2 - 14.0
14.0 - 7.0
7.0 - 4.8
Kilometers
0 5 10 20 30 40
D
DEPTH (m)
81.7 - 74.9
74.9 - 68.1
68.1 - 61.3
61.3 - 53.0
53.0 - 41.9
41.9 - 20.4
Kilometers
0 5 10 20 30 40
E
Depth (m)
36 - 65
6 - 16
25 - 36
16 - 25
Kilometers
0 5 10 20 30 40
F
Potential
Very Low
Very High
Low
High
Extremely Low
Extremely High
Kilometers
0 5 10 20 30 40
N
S
E
W

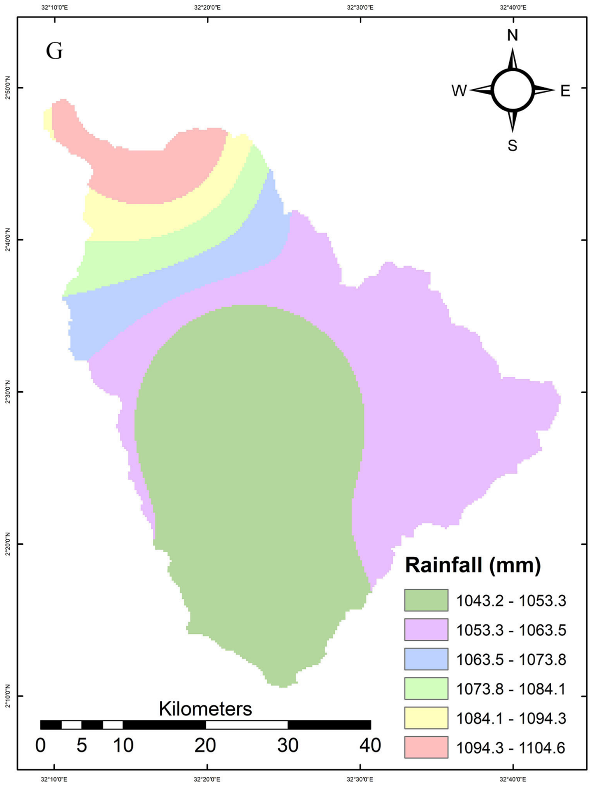

Figure 2. Map of soil (A), laterite (B), saprolite (C), granite (D), groundwater table (E), land use (F), and rainfall (G).

2) Unsegregated Lithology

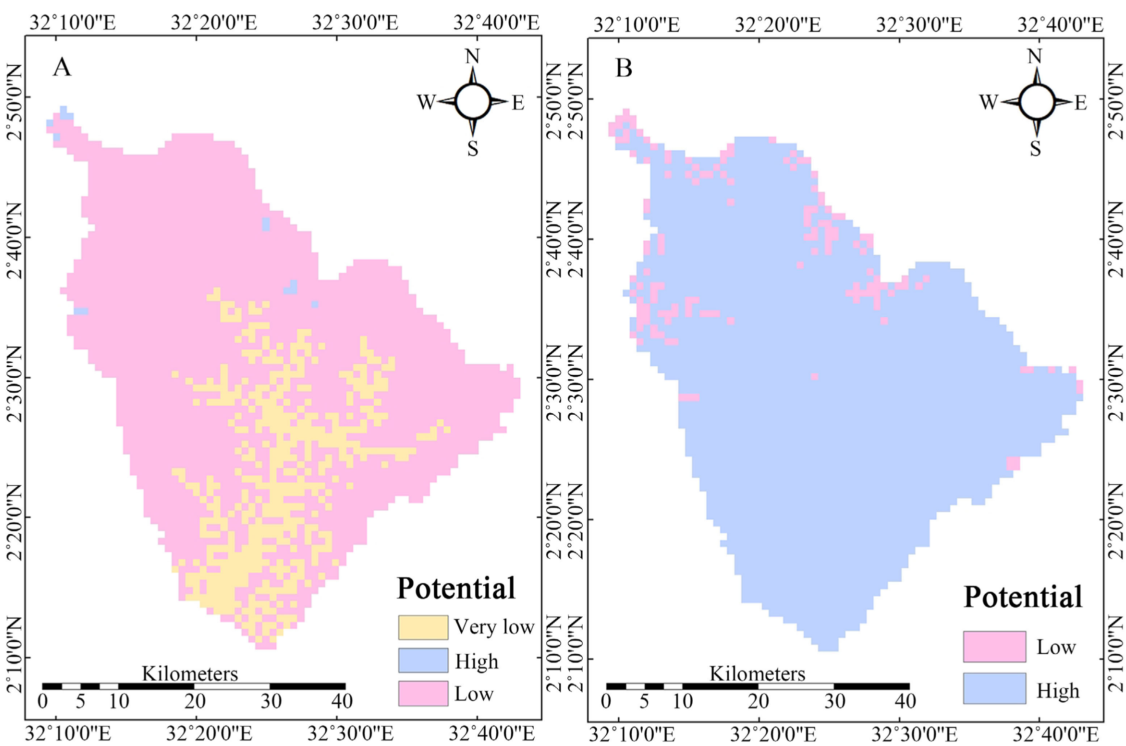

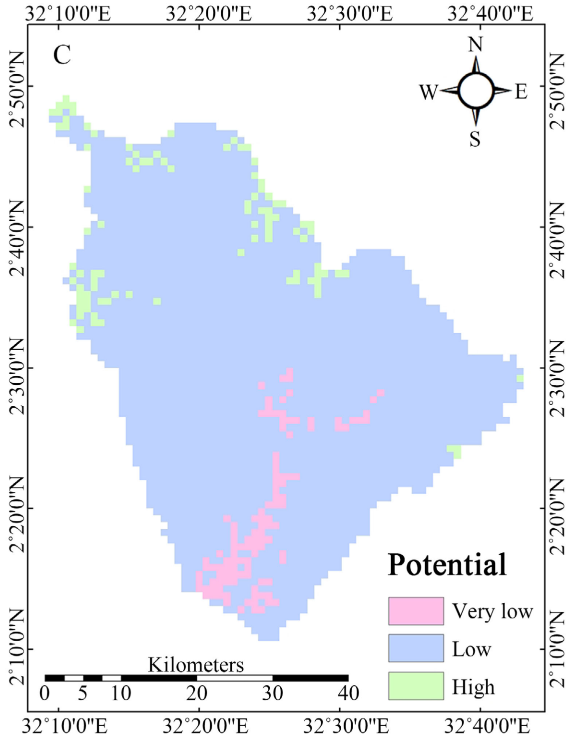

Figure 3. Map showing unsegregated lithology (Amuru group (A), gneissic granitoids of Uganda (B), and metagabbro (C)).

Unsegregated lithological units consisted of the Amuru group, Gneissic granitoids of Uganda, and Metagabbro as presented in Figure 3. The percentage spatial coverage by vulnerability potential is presented in Table 3. Gneissic granitoids dominate most parts of the watershed, and Metagabbro occupies the least area.

Table 3. Percentage spatial coverage of lithology by vulnerability classes.

Vulnerability potential	Amuru group (%)	Gneissic granitoids (%)	Metagabbro (%)
High	0.5	94.6	3.6
Low	82.2	5.4	92.2
Very low	17.3	0	4.2

5.2. Aquifer Vulnerability

The aquifer vulnerability map generated using segregated lithology is shown in Figure 4. Vulnerability was classified into high, low, and very low categories, covering 31.2%, 67.4%, and 1.4% of the watershed, respectively. Highly vulnerable regions were predominantly located towards the watershed outlet, characterized by the lowest elevations. Subsistence agriculture was the most dominant land use across all vulnerability classes (Table 4).

The vulnerability map produced using unsegregated lithology is presented in Figure 5. This map classified vulnerability as high (18.5%), low (64.3%), and very low (17.2%). A one-sample test indicated that the vulnerability maps produced by the segregated and unsegregated lithology methods were statistically different (P > chi-square = 0) (Table 5).

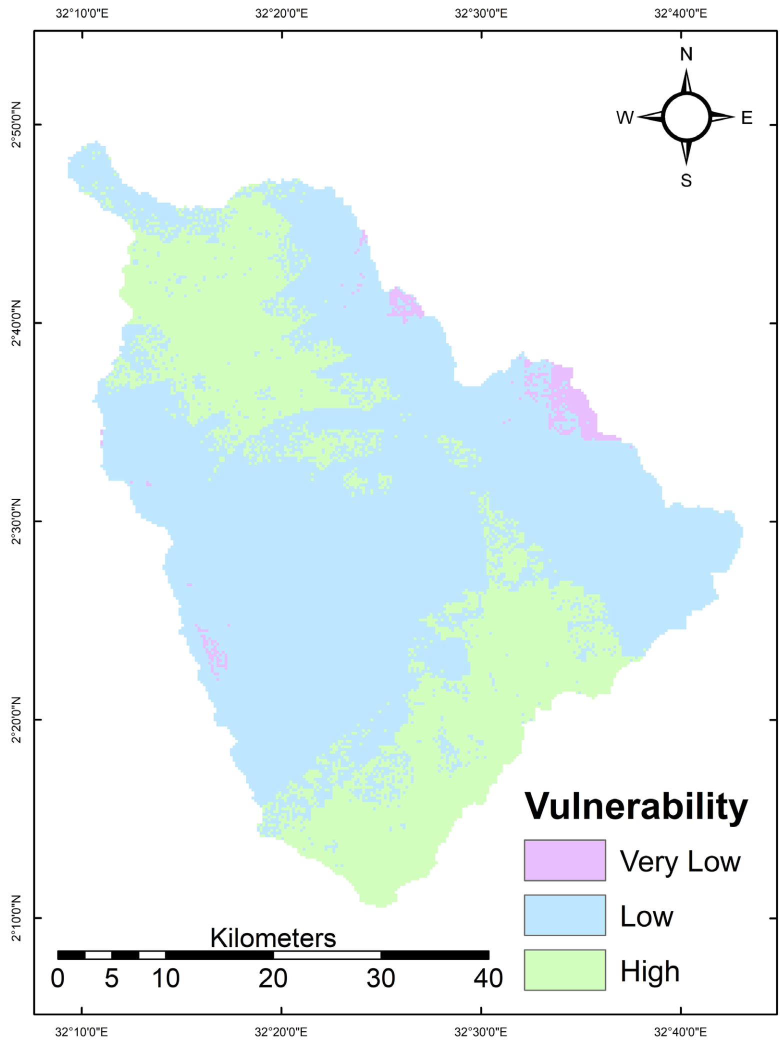

Figure 4. Map showing aquifer vulnerability using segregated lithology.

Table 4. Table showing the percentage coverage of land use within vulnerability classes.

Vulnerability	Land use category	Spatial coverage
High	Subsistence agriculture	45.1
	Rangeland	12.7
	Built up land	2.4
	Wetland	36.1
	Plantation forest	0.6
	Natural forest	3.1
Low	Subsistence agriculture	51
	Rangeland	10.9

Continued

	Built up land	1.5
	Wetland	33.8
	Plantation forest	0.5
	Natural forest	2.3
Very low	Subsistence agriculture	41.3
	Rangeland	15.8
	Built up land	1.3
	Wetland	39.4
	Plantation forest	0.1
	Natural forest	2.1

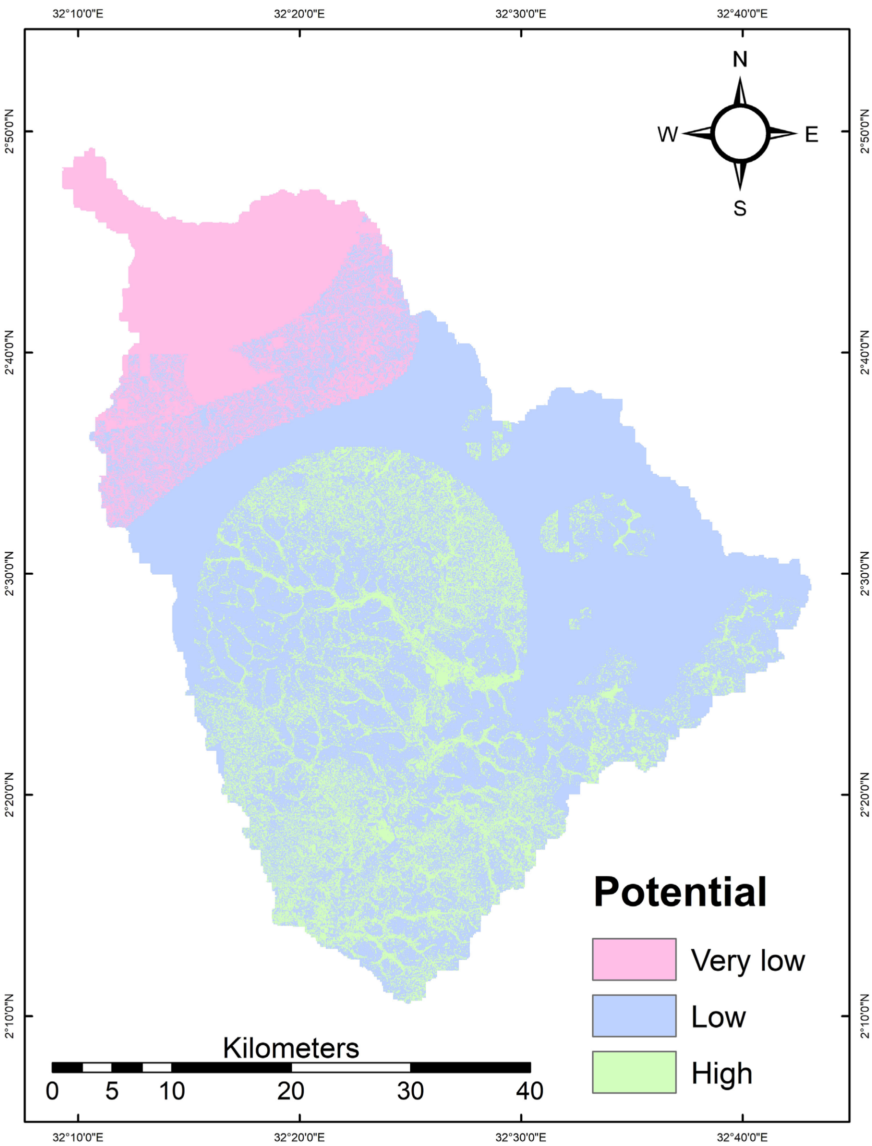

Figure 5. Map showing aquifer vulnerability using unsegregated lithology.

Table 5. Table showing variation among vulnerability maps produced using different methods.

Vulnerability map	N	mean	SD	Variance	Chi-square	DF	Prob > chi-square
Segregated lithology used	3	33.3	33.05	1092.4	2184.83	2	0
Unsegregated lithology used	3	33.3	26.83	719.6	1439.25	2	0

5.3. Accuracy of Vulnerability Map

Groundwater Quality Index (GQI) presented in **Table 6** was used to assess vulnerability map accuracy viewed as risk zones (high, low, and very low). The overlay of the groundwater quality risk potential of the 27 boreholes onto the vulnerability map produced its spatial distribution within the vulnerability category as presented in **Table 7**. The distribution in **Table 7** was used for further statistical analysis. This enabled the vulnerability map to be viewed as risk zones. As a percentage, the risk was distributed as follows: 7.4% of boreholes were within the high vulnerability category, 22% in low vulnerability, and 70.6% in very low vulnerability.

Table 6. Table showing the GQI of boreholes within the watershed.

Water Point Name	**Latitude**	**Longitude**	**DWD Number**	**GQI**	**Groundwater Quality Class (Brown *et al.*, 1972)**
Rwot Omia	441,315	287,784	38,080	250.32	**(IV):** High Risk
Keto Community School	434,514	290,856	39,288	17.23	**(I):** Very Low Risk
Te Opoko TC	444,651	268,658	38,481	27.13	**(II):** Low Risk
Ogeny Lao B	452,649	265,135	38,482	24.41	**(I):** Very low risk
Ototong PS	450,736	276,303	25,123	24.41	**(I):** Very low risk
Kamdini TC	426,445.66	247,982.42	25,129	14.28	**(I):** Very low risk
Teilwa	438,042	267,578	38,476	12.03	**(I):** Very low risk
Amwateduka	429,819	272,124	19,648	25.74	**(II):** Low Risk
Ayom Neni	450,395	279,103	38,485	23.81	**(I):** Very low risk
Langwiro	418,351.46	292,766.87	39,292	27.08	**(II):** Low risk
western ward	442,991	263,485	37,964	27.08	**(II):** Low Risk
ceng pe puru	445,237	259,458	38,479	22.41	**(I):** Very low risk
Abongowobi	445,445	259,657	38,484	23.04	**(I):** Very low risk
Laminlawino	418,150	293,155	31,206	41.73	**(II):** Low risk
Kulu Togo Peya	411,657	292,867	39,289	18.77	**(I):** Very low risk
Ayom Lony	437,669	282,977	38,081	12.45	**(I):** Very low risk
Ngai P/s	444,566.4	274,159.3	24,483	9.60	**(I):** Very low risk
Okotowe Annex P/S	454,873.13	271,159.44	24,482	8.70	**(I):** Very Low risk
Agobadong P/S	454,410	266,282	24,480	5.80	**(I):** Very low risk
Omac P/S	438,616	270,571	18,630	10.80	**(I):** Very low risk

Continued

Aleka P/S	412,979	283,267	18,631	99.00	**(IV):** High risk
Adit IDP camp	431,316	271,545	25,130	11.80	**(I):** Very low risk
Olula A	434,549	281,892	38,765	9.60	**(I):** Very Low Risk
Otelkero (Abuga)	415,172	302,843	39,294	7.70	**(I):** Very low risk
Oluba dog Tochi	416,702.51	298,603.16	39,295	8.20	**(I):** Very low risk
Aol A	450,774	278,316	46,589	23.10	**(I):** Very low risk
Akere	454,728	272,247	37,153	7.70	**(I):** Very low risk

Table 7. Table showing the GQI of boreholes by vulnerability category.

Vulnerability map	High		Low		Very low	
	Borehole name	**GQI**	**Borehole name**	**GQI**	**Borehole name**	**GQI**
Segregated lithology used	Kamdini TC	14.28	western ward	27.08		
	ceng pe puru	22.41	Ogeny Lao B	24.41		
	Abongowobi	23.04	Amwateduka	25.74		
	Te Opoko TC	27.13	Adit IDP camp	11.8		
	Agobadong P/S	5.8	Omac P/S	10.8		
	Laminlawino	41.73	Teilwa	12.03		
	Langwiro	27.08	Ngai P/s	9.6		
	Oluba dog Tochi	8.2	Olula A	9.6		
	Otelkero (Abuga)	7.7	Ayom Lony	12.45		
			Ayom Neni	23.81		
			Aol A	23.1		
			Ototong PS	24.41		
			Akere	7.7		
			Okotowe Annex P/S	8.7		
			Rwot Omia	250.32		
			Keto Community School	17.23		
			Aleka P/S	99		
			Kulu Togo Peya	18.77		
Unsegregated lithology used	Teilwa	12.03	Kamdini TC	14.28	Laminlawino	41.73
	Ngai P/s	9.6	ceng pe puru	22.41	Langwiro	27.08
			Abongowobi	23.04	Oluba dog Tochi	8.2
			western ward	27.08	Otelkero (Abuga)	7.7
			Omac P/S	10.8		
			Amwateduka	25.74		
			Adit IDP camp	11.8		
			Te Opoko TC	27.13		

Continued

Agobadong P/S	5.5
Ogeny Lao B	24.41
Okotowe Annex P/S	8.7
Akere	7.7
Ototong PS	24.41
Aol A	23.1
Ayom Neni	23.81
Rwot Omia	250.32
Olula A	9.6
Ayom Lony	12.45
Keto Community School	17.23
Aleka P/S	99
Kulu Togo Peya	18.77

A one-sample t-test revealed a significant difference within the vulnerability classes (p-value = 0.0295) when comparing the two methods (Table 8). However, no significant difference was found within the low vulnerability class (p-value = 0.47). Analysis for the very low vulnerability class was not performed due to the absence of wells within this category. The analysis also revealed distinct partitioning of vulnerability classes, especially in the high vulnerability category, as presented in Table 9.

Table 8. The table shows the level of vulnerability by class for the map produced using segregated and unsegregated lithology.

Vulnerability class	Test parameters	Segregated lithology	Unsegregated lithology
High	mean	19.7	10.8
	Standard deviation	9	2
	Degree of freedom	9	
	P (T <= t)	**0.0295**	
Low	mean	34.3	32.7
	Standard deviation	18	21
	Degree of freedom	35	
	P (T <= t)	**0.47**	

Table 9. The table shows vulnerability partitioning between the two methods.

Vulnerability classes	Lithology type used	t-statistics	DF	Prob > t
High	Segregated lithology	5.01404	8	0.00103
	Unsegregated lithology	8.90123	1	0.07122
Low	Segregated lithology	2.51954	17	0.02205
	Unsegregated lithology	2.81064	20	0.0108

The Area Under the Curve (AUC) analysis by vulnerability potential is presented in **Table 10**. Vulnerability maps produced using segregated lithology showed higher accuracy than their counterpart produced using unsegregated lithology.

Table 10. Table showing mapping accuracy between the two methods.

Vulnerability Potential	Segregated lithology	Unsegregated lithology
High	0.75	-
Low	1	0.275

Further AUC analysis of vulnerability by category produced using segregated lithology revealed an accuracy of 75% for high vulnerability potential and 100% for low vulnerability potential.

6. Discussion

Aquifer contamination is a complex issue driven by various factors, including surface waste, geochemical processes, and their combined effects [15]. Anthropogenic activities and land use patterns are widely recognized for their negative impact on groundwater quality [16] [17]. In the Tochi watershed, our Groundwater Quality Index (GQI) analysis indicated that 70.6% of boreholes fall within the very low-risk category, and 22% within the low-risk category, suggesting that the water sources within the period March 2003 to December 2016 were generally safe for use. However, this may not be the case in the current year, 2026, due to the cumulative effect of contaminants in soil arising from anthropogenic activities.

Aquifer depth plays a critical role in natural water purification by providing sufficient residence time for contaminant attenuation during infiltration. However, the presence of shallow groundwater tables (<35 m) in high vulnerability regions, particularly when coupled with intense rainfall, can significantly increase the likelihood of contaminants reaching the groundwater directly [18]. Previous studies in Uganda have shown that most aquifers are semi-confined, with depths typically ranging from 27 m to 35 m [19]. This semi-confined nature renders them susceptible to pollution from external sources [20] [21]. Indeed, surface-derived groundwater contamination, including elevated levels of total coliform, nitrate, and sulphate, has been reported in Gulu district within similar semi-confined aquifer depths (12 m to 76 m) [15]. These findings underscore the urgent need for effective intervention strategies to mitigate future groundwater contamination risks.

This study advanced aquifer vulnerability mapping by comparing two methodologies: one incorporating segregated subsurface lithology and another using unsegregated lithology, alongside other influencing factors. The vulnerability maps, classified into high, low, and very low risk, were statistically different between the two methods (P > chi-square = 0 at $\alpha = 0.05\%$). This significant difference highlights the potential impact of lithological detail on vulnerability assessment in addition to the potential contribution of AHP weight and criteria.

Specifically, the segregated lithology approach yielded a statistically significant improvement in delineating high vulnerability zones compared to the unsegregated lithology (p-value = 0.0295). This enhanced performance is likely attributable to the method's ability to capture the intricate variations in hydraulic properties and flow paths within distinct subsurface layers (soil, laterite, saprolite, granite). The observed differences can further be investigated by focusing on the interplay between lithological details, AHP weight, and criteria for a better conclusion. In spite of the contribution of other factors in vulnerability mapping, the existence of significant elevation differences, which encourage flow convergence zones, is more accurately represented when lithology is disaggregated, allowing for a more precise identification of high-risk areas. For instance, laterite, with its highly variable hydraulic conductivity and dual-porosity characteristics, facilitates faster horizontal water movement along relict bedrock foliation planes and fractures [22]. By segregating such layers, the model better reflects the actual flow dynamics. In contrast, the unsegregated approach, which lumps these layers into broader geological units, may oversimplify the subsurface hydrogeology, leading to less accurate vulnerability predictions.

Within the low vulnerability class, the accuracy of the two methods did not vary significantly (P-value = 0.47). This suggests that for areas with inherently low vulnerability, the level of lithological detail might have a less pronounced impact on the overall assessment. However, the one-sample t-test performed on vulnerability classes for segregated lithology further confirmed that the vulnerability potential matched the associated risk levels derived from the GQI (p-value=0.00103 for high potential and p-value=0.02205 for low potential). The high AUC values (75% for high vulnerability potential and 100% for low vulnerability potential) further affirm the robustness and accuracy of the segregated lithology approach in mapping aquifer vulnerability. This aligns with studies by Zghibi *et al.* (2016), who emphasized the role of hydrogeological system properties, particularly hydraulic conductivity and aquifer medium, as primary intrinsic factors influencing aquifer vulnerability. By segmenting the aquifer thickness into units with more uniform textural characteristics, our method effectively assessed the contribution of varying subsurface topology gradients to identify potential flow convergence zones, leading to improved vulnerability mapping. [23]

7. Conclusions

This study successfully compared two methodologies for aquifer vulnerability mapping in the Tochi watershed, utilizing factors such as groundwater table, rainfall, land use, and both segregated (soil, laterite, saprolite, granite) and unsegregated (Amuru group, gneissic granitoids, metagabbro) lithological data. The primary objective was to demonstrate the improved accuracy achieved by integrating segregated lithology compared to a single unsegregated lithology thematic map.

Our analysis, validated against the Groundwater Quality Index (GQI) of boreholes, unequivocally demonstrated that the two methods produced statistically different vulnerability maps. Crucially, the segregated lithology approach resulted in a significantly better prediction within the high vulnerability map categories (p-value = 0.0295). This improvement is partly attributed to the enhanced refinement in subsurface lithology, achieved by separating geological units into autonomous layers during the mapping process, which more accurately reflects complex hydrogeological conditions. Furthermore, the variations within the GQI were effectively partitioned according to the vulnerability classes, reinforcing the contribution of segregated lithology to improved accuracy (p-values of 0.00103 for high and 0.02205 for low vulnerability classes, respectively).

While the GQI currently indicates that the majority of water sources in the watershed are safe for use for the period March 2003 to December 2016 (22% low risk and 70.6% very low risk), the prevalence of semi-confined aquifer systems and the projected population growth in Uganda pose significant future risks. The existing mixed land use patterns further necessitate proactive management interventions to prevent future aquifer pollution. Therefore, the adoption of methodologies that incorporate detailed subsurface stratification, such as the segregated lithology approach presented here, is crucial for developing more accurate vulnerability maps and ensuring sustainable groundwater resource management.

8. Recommendations

To further enhance the accuracy and applicability of aquifer vulnerability models, the following areas warrant future investigation:

1) Production of Subsurface models: More borehole wells should be used in the development of the subsurface model to reduce interpolation error for better identification of flow convergence zones.

2) Incorporation of Fissures and Fractures: The current segregated lithology model assumes a continuous subsurface, with limited explicit attention given to fissures, particularly within the granite layer. Future studies should explore advanced modeling techniques to incorporate the spatial distribution and hydraulic properties of such features, as they can significantly influence groundwater flow and contaminant transport, especially in fractured bedrock environments. The coincidence of strike-slip faults with the lowest elevations in this study, creating flow convergence zones, highlights the importance of these structural features, which may vary across different watersheds.

3) AHP weights, criteria, and segregated lithology: Further research is needed to quantify the individual contribution of AHP weights, criteria, and segregated lithology to aquifer vulnerability mapping.

4) Advanced Land Surface Modeling: Given the shallow depth to the groundwater table in some locations and the semi-confined nature of the aquifer systems, detailed land surface modeling should be considered. This would involve integrating more dynamic representations of infiltration, runoff, and pollutant loading from various land use types. Such models could provide a more comprehensive understanding of contaminant pathways and aid in developing preventative measures to avert future contamination of the aquifer systems, particularly in light of the mixed land use within the watershed.

Acknowledgements

The authors extend their sincere gratitude to the district water officers of Gulu, Oyam, Omoro, Nwoya, and Apac for providing the borehole drill logs essential for developing the segregated lithology maps. Appreciation is also extended to the Ministry of Energy and Mineral Development for making available the Geology Map of Uganda, which was instrumental in this study.

Author Contributions

Conceptualization, Joachim Bongomin and Martine Nyeko; methodology, Joachim Bongomin and Martine Nyeko; software, Joachim Bongomin and Martine Nyeko; validation, Joachim Bongomin, Martine Nyeko, and Denis Nono; formal analysis, Joachim Bongomin, Martine Nyeko, Denis Nono, and Byakatonda Jimmy; investigation, Joachim Bongomin, Martine Nyeko, Denis Nono, Byakatonda Jimmy, Geoffrey Openy, Richard Louis Labeja; resources, Joachim Bongomin, Martine Nyeko, Denis Nono, Byakatonda Jimmy, Geoffrey Openy, Richard Louis Labeja; data curation, Joachim Bongomin and Martine Nyeko; writing—original draft preparation, Joachim Bongomin, Martine Nyeko, and Denis Nono; writing—review and editing, Joachim Bongomin, Martine Nyeko, Denis Nono, Byakatonda Jimmy, Geoffrey Openy, Richard Louis Labeja; visualization, Joachim Bongomin, Martine Nyeko, Denis Nono, Byakatonda Jimmy, Geoffrey Openy, Richard Louis Labeja; supervision, Joachim Bongomin, Martine Nyeko, Denis Nono, Byakatonda Jimmy, Geoffrey Openy, Richard Louis Labeja; project administration, Joachim Bongomin, Martine Nyeko, Denis Nono, Byakatonda Jimmy, Geoffrey Openy, Richard Louis Labeja; funding acquisition, Joachim Bongomin. All authors have read and agreed to the published version of the manuscript.

Conflicts of Interest

The authors declare no conflicts of interest regarding the publication of this paper.

References

[1] Shinwari, F.U., Khan, M.A., Siyar, S.M., Liaquat, U., Kontakiotis, G., Zhran, M., *et al.* (2025) Evaluating the Contamination Susceptibility of Groundwater Resources through Anthropogenic Activities in Islamabad, Pakistan: A GIS-Based DRASTIC Approach. *Applied Water Science*, **15**, Article No. 81. https://doi.org/10.1007/s13201-025-02374-9

[2] Davamani, V., John, J.E., Poornachandhra, C., Gopalakrishnan, B., Arulmani, S., Parameswari, E., *et al.* (2024) A Critical Review of Climate Change Impacts on Groundwater Resources: A Focus on the Current Status, Future Possibilities, and Role of Simulation Models. *Atmosphere*, **15**, Article No. 122.

https://doi.org/10.3390/atmos15010122

[3] Abu-Bakr, H.A.e. (2020) Groundwater Vulnerability Assessment in Different Types of Aquifers. *Agricultural Water Management*, **240**, Article ID: 106275. https://doi.org/10.1016/j.agwat.2020.106275

[4] Khosravi, K., Bordbar, M., Paryani, S., Saco, P.M. and Kazakis, N. (2021) New Hybrid-Based Approach for Improving the Accuracy of Coastal Aquifer Vulnerability Assessment Maps. *Science of the Total Environment*, **767**, Article ID: 145416. https://doi.org/10.1016/j.scitotenv.2021.145416

[5] Medici, G., Smeraglia, L., Torabi, A. and Botter, C. (2021) Review of Modeling Approaches to Groundwater Flow in Deformed Carbonate Aquifers. *Groundwater*, **59**, 334-351. https://doi.org/10.1111/gwat.13069

[6] Saranya, T. and Saravanan, S. (2022) Assessment of Groundwater Vulnerability Using Analytical Hierarchy Process and Evidential Belief Function with DRASTIC Parameters, Cuddalore, India. *International Journal of Environmental Science and Technology*, **20**, 1837-1856. https://doi.org/10.1007/s13762-022-03944-z

[7] Gogu, R.C., Hallet, V. and Dassargues, A. (2003) Comparison of Aquifer Vulnerability Assessment Techniques. Application to the Néblon River Basin (Belgium). *Environmental Geology*, **44**, 881-892. https://doi.org/10.1007/s00254-003-0842-x

[8] Jang, C.S., Lin, C.W., Liang, C.P. and Chen, J.S. (2015) Developing a Reliable Model for Aquifer Vulnerability. *Stochastic Environmental Research and Risk Assessment*, **30**, 175-187. https://doi.org/10.1007/s00477-015-1063-z

[9] Joachim, B., Geoffrey, O., Denis, N., Jimmy, B., Louis, L.R. and Martine, N. (2025) Application of Geomodeller in Production of Enhanced Lithological Map for Groundwater Exploration. *Cureus Journal of Engineering*, **2**, es44388-025-05364-4. https://doi.org/10.7759/s44388-025-05364-4

[10] MW&E (2017) Uganda Water Atlas. https://www.mwe.go.ug

[11] Opio, C. (2010) Biological and Physical Characteristics of Drinking Water from Wells in Kamdini Parish, Northern Uganda. Research Extension Note Number 6. http://www.unbc.ca/nres/research_extension_notes.html

[12] Okot-Okumu, J. and Otim, J. (2015) The Quality of Drinking Water Used by the Communities in Some Regions of Uganda. *International Journal of Biological and Chemical Sciences*, **9**, Article No. 552. https://doi.org/10.4314/ijbcs.v9i1.47

[13] Opio, C. and Hurst, C. (2012) Building Effective Drinking Water Management Policies in Rural Africa: Lessons from Northern Uganda. http://www.jstor.com/stable/resrep16139

[14] Saaty, T.L. (2008) Decision Making with the Analytic Hierarchy Process. *International Journal of Services Sciences*, **1**, 83-98.

[15] Wilson, G.J.L., Muloogi, D., Hamisi, R., Denwood, T., Bhattacharya, P., Nuwategeka, E., *et al.* (2024) Surface-Derived Groundwater Contamination in Gulu District, Uganda: Chemical and Microbial Tracers. *Science of the Total Environment*, **955**, Article ID: 177118. https://doi.org/10.1016/j.scitotenv.2024.177118

[16] Liu, X., Wang, X., Zhang, L., Fan, W., Yang, C., Li, E., *et al.* (2021) Impact of Land Use on Shallow Groundwater Quality Characteristics Associated with Human Health Risks in a Typical Agricultural Area in Central China. *Environmental Science and Pollution Research*, **28**, 1712-1724. https://doi.org/10.1007/s11356-020-10492-x

[17] Goswami, S. and Rai, A.K. (2023) Impact of Anthropogenic and Land Use Pattern Change on Spatio-Temporal Variations of Groundwater Quality in Odisha, India. *Environmental Science and Pollution Research*, **30**, 101483-101500.

https://doi.org/10.1007/s11356-023-29372-1

[18] Chen, I., Chang, L. and Chang, F. (2018) Exploring the Spatio-Temporal Interrelation between Groundwater and Surface Water by Using the Self-Organizing Maps. *Journal of Hydrology*, **556**, 131-142. https://doi.org/10.1016/j.jhydrol.2017.10.015

[19] Owor, M., Muwanga, A., Tindimugaya, C. and Taylor, R.G. (2021) Hydrogeochemical Processes in Groundwater in Uganda: A National-Scale Analysis. *Journal of African Earth Sciences*, **175**, Article ID: 104113. https://doi.org/10.1016/j.jafrearsci.2021.104113

[20] Jia, Z., Bian, J. and Wang, Y. (2018) Impacts of Urban Land Use on the Spatial Distribution of Groundwater Pollution, Harbin City, Northeast China. *Journal of Contaminant Hydrology*, **215**, 29-38. https://doi.org/10.1016/j.jconhyd.2018.06.005

[21] Nyenje, P.M., Ocoromac, D., Tumwesige, S., Ascott, M.J., Sorensen, J.P.R., Newell, A.J., *et al*. (2022) Hydrogeology of an Urban Weathered Basement Aquifer in Kampala, Uganda. *Hydrogeology Journal*, **30**, 1469-1487. https://doi.org/10.1007/s10040-022-02474-9

[22] Willis, D.W. (2004) Field Hydrogeology. McGraw-Hill Companies, Inc.

[23] Zghibi, A., Merzougui, A., Chenini, I., Ergaieg, K., Zouhri, L. and Tarhouni, J. (2016) Groundwater Vulnerability Analysis of Tunisian Coastal Aquifer: An Application of DRASTIC Index Method in GIS Environment. *Groundwater for Sustainable Development*, **2**, 169-181. https://doi.org/10.1016/j.gsd.2016.10.001